Interactions between Ice-Albedo, Lapse-Rate and Cloud-Top Feedbacks: An Analysis of the Nonlinear Response of a GCM Climate Model

V. RAMANATHAN

National Center for Atmospheric Research,[1] Boulder, Colo. 80307

(Manuscript received 13 May 1977, in revised form 29 August)

ABSTRACT

This paper examines the interactions between ice-albedo, lapse-rate and cloud-top feedbacks with the aid of GCM climate experiments published by Wetherald and Manabe (1975). First we establish that the longwave modification effect (the so-called "greenhouse effect") of clouds depends largely on the temperature difference T_{sc} between surface and cloud tops. If T_{sc} changes with a change in the surface temperature T_s, then the longwave modification effect of clouds would change which would result in a modification of the initial change in T_s. This feedback between the longwave modification effect of clouds and T_s is referred to as the cloud top feedback in this paper. The sign of this feedback is considered positive (negative) when it amplifies (decreases) an initial change in T_s and it is shown that the sign is determined by the sign of dT_{sc}/dT_s.

In the GCM climate experiments of Wetherald and Manabe (1975), $dT_{sc}/dT_s<0$ at low latitudes and $dT_{sc}/dT_s>0$ at high latitudes; consequently, cloud tops exert a positive feedback at high latitudes and a negative feedback at low latitudes. We then demonstrate that the interaction between cloud-top, ice-albedo and lapse-rate feedbacks induces a nonlinear response of surface temperature changes in a GCM climate model.

The significance of the H_2O *e*-type absorption to the surface energy budget of the tropics is stressed. The results suggest that the *e*-type absorption will be important in determining the sensitivity of the hydrological cycle to changes in surface temperature.

1. Introduction

The interactions between the four basic components of the earth's climate system (i.e., the surface, hydrosphere, atmosphere and cryosphere) give rise to a myriad of feedbacks which are so numerous that as yet we have been unable to reliably estimate either their individual or their collective influence on the climate. A quantitative understanding of these feedback processes is crucial for estimating the sensitivity of the climate to changes in the climate governing parameters. This includes changes in solar constant, orbital parameters, and optically active constituents (i.e., CO_2, H_2O, O_3 and aerosols)—several other possibilities exist.

Schneider and Dickinson (1974) have reviewed the various feedbacks that have been identified thus far. The present paper examines the connections between some of these feedbacks and reports the existence of a possible coupling between ice-albedo, lapse-rate and cloud-top radiative interactions. The analysis reported here also suggests that this coupling can induce a nonlinear response of the surface temperature T_s to changes in the climate governing parameters.

A general circulation model (GCM) of the climate is used in the analysis. In particular, we consider here GFDL's GCM developed by Manabe (1969), primarily because this model can compute T_s and has been used to perform several interesting climate change experiments. The particular experiment of interest is the recently reported work of Wetherald and Manabe (1975) in which these authors examined the response of the GCM climate to changes in the solar constant. Their result for the change in global $\bar{T}_s$ as a function of the change in solar constant, which is shown in Table 1, reveals an interesting aspect of climate sensitivity. Restricting our attention initially to columns 1 and 2 in the table, we see that the surface temperature change $\Delta\bar{T}_s$ is nonlinear with respect to changes in the solar constant. In general, the magnitude of $\Delta\bar{T}_s$ is larger for a solar constant decrease than for an increase. Wetherald and Manabe (1975, hereafter referred to as WM) have performed a detailed analysis of their experiments and suggest that the nonlinearity is largely due to the ice-albedo feedback operating as follows: As T_s increases (or decreases) the ice cover shrinks toward polar regions (or expands toward midlatitudes) which reduces (or increases) the global albedo and this reduction (or increase) in the albedo causes an additional increase (or decrease) in $\bar{T}_s$. Thus the ice-albedo provides a positive feedback. The nonlinearity in this feedback is believed due to the

[1] The National Center for Atmospheric Research is sponsored by the National Science Foundation.

TABLE 1. Changes in the earth's global surface temperature resulting from changes in solar constant: GCM, general circulation model; RCM, radiative-convective model; $\bar{T}_s$, global surface temperature; S_0, solar constant; α_p, planetary albedo; $\bar{F}$, planetary outgoing longwave flux at the top of the atmosphere. The results for $\Delta\bar{T}_s$ and $\Delta\bar{F}$ are taken from Wetherald and Manabe (1975). $\Delta\alpha_p$ is calculated from the values of reflected solar flux (global values) given in Wetherald and Manabe (1975).

Experiment no.	Change of solar constant (%)	GCM results $\Delta\bar{T}_s$ (K)	$\Delta\alpha_p$	$\frac{\Delta\alpha_p}{\Delta\bar{T}_s}$	$\Delta\bar{F}$ (W m^{-2})	$\frac{\Delta\bar{F}}{\Delta\bar{T}_s}$	RCM results $\Delta\bar{T}_s$ (K)
1	$0\rightarrow+2$	+3.04	−0.0046	−0.0015	6.28	2.07	+2.57
2	$0\rightarrow-2$	−4.37	+0.0068	−0.0016	−6.98	1.59	−2.55
3	$-2\rightarrow-4$	−5.71	+0.0154	−0.0027	−9.77	1.7	−2.54

expansion (or contraction) of the ice cover as T_s is increased (or decreased). We will examine this feedback from the equations for global energy balance and the global sensitivity parameter $\beta=S_0(d\bar{T}_s/dS)$, as defined by Schneider and Mass (1975), where S is the solar constant with $S_0=1360$ W m^{-2} denoting the current solar constant:

$$\bar{F}=(S/4)(1-\alpha_p), \tag{1}$$

$$\beta=S_0\frac{d\bar{T}_s}{dS}=\frac{\bar{F}_0}{(d\bar{F}/d\bar{T}_s)+[(S_0/4)(d\alpha_p/d\bar{T}_s)]}, \tag{2}$$

where α_p is the albedo, $\bar{F}$ the outgoing longwave flux and $\bar{F}_0$ the value of $\bar{F}$ corresponding to S_0. Eq. (1) is the global energy balance equation and Eq. (2) was derived by Cess (1976) from Eq. (1).

The ice-albedo feedback manifests itself through the $d\alpha_p/d\bar{T}_s$ term. From Table 1, it is seen that $d\alpha_p/d\bar{T}_s$ is essentially a constant for the first two experiments, i.e., when S_0 is increased and decreased by 2%. Thus we conclude that the nonlinear response in $\Delta\bar{T}_s$ between experiments 1 and 2 cannot be primarily due to the ice albedo feedback.

We now compare the longwave sensitivity parameter $d\bar{F}/d\bar{T}_s$ ($=\Delta\bar{F}/\Delta\bar{T}_s$ which is shown in Table 1) between the two experiments. We see that $d\bar{F}/d\bar{T}_s$ is substantially different between the two experiments and furthermore this difference explains most of the nonlinear response of the two experiments. Introducing WM's values of $\Delta\alpha_p/\Delta\bar{T}_s$ and $\Delta\bar{F}/\Delta\bar{T}_s$ in Eq. (2), we obtain

$$\beta=\begin{cases}150\text{ K}, & \text{Exp. 1}\\ 220\text{ K}, & \text{Exp. 2}\end{cases} \tag{3}$$

The value of $\beta=150$ K corresponds, of course, to $\Delta\bar{T}_s=1.5$ K for a 1% change in solar constant. Eq. (3) indicates that $\Delta\bar{T}_s=3$ K for experiment 1 and $\Delta\bar{T}_s=4.4$ K for experiment 2 which agrees exactly with the values of $\Delta\bar{T}_s$ shown in Table 1. Next, comparing experiments 2 and 3, we see that the nonlinear change in $\Delta\bar{T}_s$ is primarily caused by the nonlinear change in $d\alpha_p/d\bar{T}_s$. From the preceding exercise we conclude that the nonlinear response of $\Delta\bar{T}_s$ between the three experiments results from the combined effect of the longwave sensitivity parameter and the albedo feedback.

We will attempt to prove that the nonlinear response of WM's GCM climate model is due to the interactions between the ice-albedo, lapse-rate and cloud-top feedbacks. We will first establish the existence of a cloud-top feedback in WM's GCM. This feedback involves the longwave modification effect (the so-called "greenhouse" effect) of clouds on T_s. It is shown in this analysis that the fundamental parameter which determines the longwave effect of clouds in the model is the difference between the surface and cloud-top temperature, $T_{sc}=T_s-T_c$, where T_c is the cloud-top temperature. In WM's GCM, the parameter T_{sc} changes as T_s is changed and consequently the modification by clouds of longwave radiation changes with T_s and this change modifies the initial change in T_s. Next, we will illustrate the interactions between the cloud-top, lapse-rate and ice-albedo feedbacks and show how these interactions determine the global sensitivity.

2. Analysis of feedback mechanisms in WM's GCM

a. Cloud-top feedback mechanism

Clouds have two competing opposite effects on T_s: their modification of albedo which tends to cool the surface and their modification of longwave radiation which tends to warm the surface. In the present discussion we are solely concerned with the longwave modification. The outgoing longwave flux F can be written explicitly as a function of the cloud cover A_c, i.e.,

$$F=c_1-A_cc_2, \tag{4}$$

where c_1 is the clear sky outgoing flux and c_2 represents the longwave modification effect of clouds. The longwave sensitivity parameter can be derived from Eq. (4) as

$$\frac{dF}{dT_s}=\frac{dc_1}{dT_s}-A_c\frac{dc_2}{dT_s}-c_2\frac{dA_c}{dT_s}. \tag{5}$$

The last term on the right-hand side of Eq. (5) denotes the cloud-cover feedback and since this

feedback is neglected in WM, we will also ignore it. As explained below, the term dc_2/dT_s gives the cloud-top feedback. A nonzero value of dc_2/dT_s implies that the modification by clouds of longwave radiation changes with a change in T_s and this change would modify the initial change in T_s. We refer to this feedback between c_2 and T_s as cloud-top feedback because, as we will show shortly, the sign and magnitude of dc_2/dT_s is essentially determined by the relationship between cloud-top temperature change and surface temperature change.

Before we attempt to estimate this term we have to identify the parameters and variables that determine the magnitude of c_2. For this purpose, we will consider the equation for c_2 [see Cess (1974) for the derivation]:

$$c_2=\sigma\left\{T_s^4[1-\epsilon(0,\infty)]-T_c^4[1-\epsilon(z_c,\infty)]-\int_0^{z_c}T^4(z)\frac{d\epsilon(z,\infty)}{dz}dz\right\}, \quad (6)$$

where σ is the Stefan-Boltzman's constant and, z the altitude, with $z=0$ and $z=\infty$ denoting the surface and the top of the atmosphere, respectively. The parameter ϵ denotes the combined wavelength-integrated emissivity of H_2O, CO_2 and O_3. Eq. (6) is derived by assuming the cloud to be black and this equation can be extended easily to clouds whose emissivity is wavelength-independent by multiplying c_2 by the cloud emissivity. If we further make the assumption that the clouds at various altitudes are uncorrelated, we can apply Eq. (6) directly to multiple cloud layers. Eq. (6) shows that c_2 depends on T_s, T_c, z_c, the atmospheric temperature profile and the vertical distribution of H_2O CO_2 and O_3 (these gases determine the magnitude of ϵ). It then follows that, the term dc_2/dT_s would depend on the functional dependence of T_c, z_c, atmospheric temperatures and humidity on T_s. Hence, we have to infer the coupling between T_s, T_c, z_c, and the atmospheric temperatures and humidity before we can attempt to evaluate the overall cloud-top feedback. This complex problem can be considerably simplified if we can identify a single parameter which practically determines the magnitude of c_2. We will now prove that such a parameter exists and that this parameter is T_s-T_c, i.e., c_2, as formulated by Eq. (6), is essentially determined by the difference between the surface and cloud-top temperature.

To arrive at this conclusion we computed c_2 for several observed profiles of atmospheric temperature and humidity. The profiles were chosen to cover the extreme values of T_s, T and humidity observed in the atmosphere. The computed values of c_2 are plotted as a function of z_c in Fig. 1. The adopted atmospheric temperature and humidity profiles corresponding to the respective curves are shown in Figs. 2 and 3. The

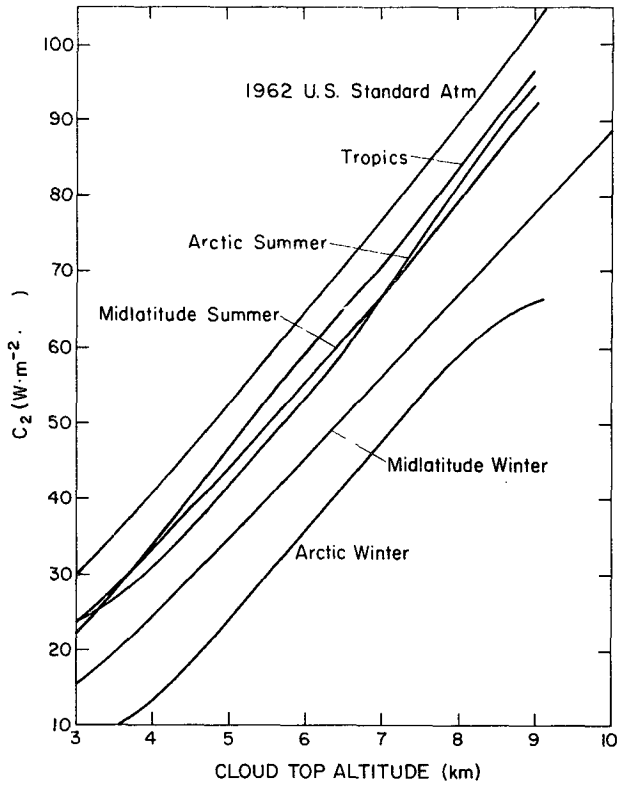

FIG. 1. Longwave modification effect of clouds as a function of cloud-top altitude. The profiles of temperature and H_2O density adopted for these calculations are shown in Figs. 2 and 3.

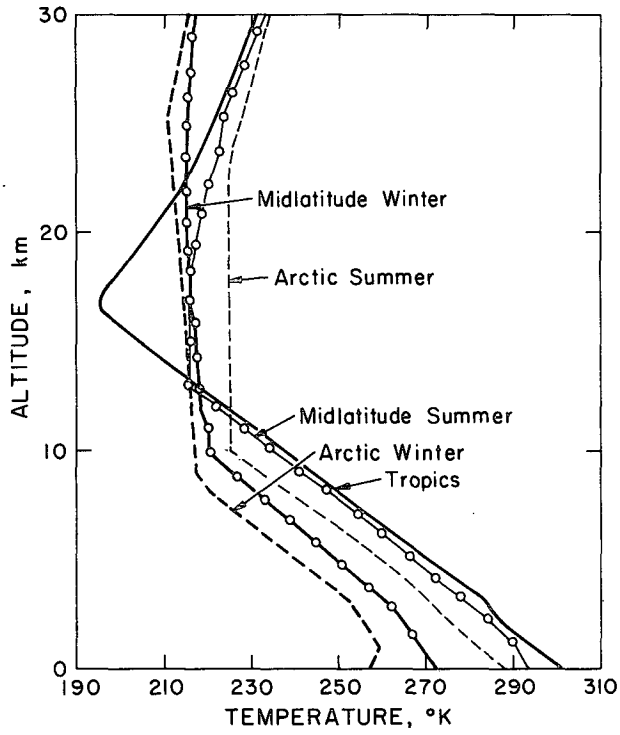

FIG. 2. Observed temperature profiles for latitudes and seasons (after McClatchey *et al.*, 1972).

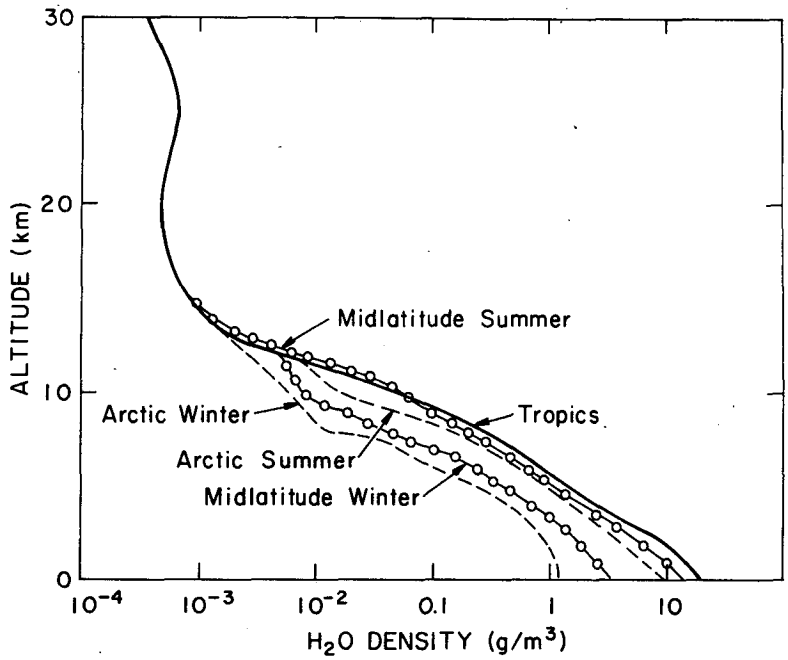

FIG. 3. Observed H_2O density profiles for latitudes and seasons (after McClatchey *et al.*, 1972).

computations for c_2 were performed with the aid of the radiative transfer model described in Ramanathan (1976). The significant difference in the magnitude and the shape between the various c_2 curves shown in Fig. 1 clearly rules out the possibility of z_c being the sole dependent variable for c_2. If z_c had been the sole dependent variable, then all of the c_2 curves shown in Fig. 1 should have collapsed into a single curve. Next, we plotted (not shown here) c_2 as a function of T_c and again there was substantial difference between the various c_2 curves. Finally, we show in Fig. 4 a plot of the computed values of c_2 as a function of T_s-T_c. The result shown in Fig. 4 demonstrates that, in spite of the significant differences in the atmospheric temperature and humidity profiles, c_2 depends essentially only on T_s-T_c and consequently we can express the term dc_2/dT_s as

$$\frac{dc_2}{dT_s}=\frac{\partial c_2}{\partial T_{sc}}\frac{dT_{sc}}{dT_s}, \tag{7}$$

where $T_{sc}=T_s-T_c$. The analysis up to this point indicates that the complex problem of estimating the cloud-top feedback may be reduced to a relatively simpler problem of estimating the term dT_{sc}/dT_s. In order to assess the validity of our conclusion that $c_2=c_2(T_{sc})$, we will first examine whether the conclusion is data- or model-dependent and then discuss the applicability of the conclusions to the currently available climate models and to the actual climate system.

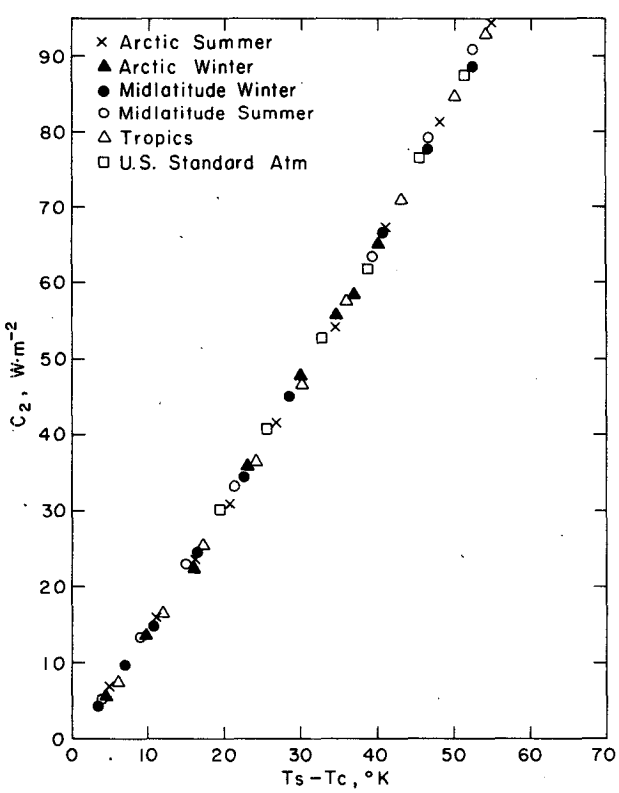

FIG. 4. Longwave modification effect of clouds as a function of $T_{sc}=T_s-T_c$, where T_s is surface temperature and T_c cloud-top temperature.

1) DATA DEPENDENCE

We computed c_2 by adopting a different set of observed data, for temperature and relative humidity, than those adopted for the results shown in Fig. 4.

The data sets used for these computations are obtained from Oort and Rasmusson (1971) and are comprised of temperature and humidity profiles at 20°N and 50°N and hemispheric mean profiles for the months of January, April and July. These additional sets of computations also indicate that c_2 is essentially a function of T_{sc}. Hence, it is reasonable to expect that our conclusion is not dependent on the particular data set used to obtain Fig. 4.

2) Model dependence

The formulation for c_2 as given by Eq. (6) employs two simplifying assumptions which are conventional in state-of-the-art climate models:

(i) The longwave emissivity of clouds is wavelength-independent. This assumption seems to be valid for the low and middle level clouds since theoretical studies of Yamamoto *et al.* (1970) and observational results reported in Allen (1971) indicate that the low and middle levels clouds are essentially black in the longwave length region. However, Platt and Gambling's (1971) and Hunt's (1973) studies indicate that this assumption may be inadequate for high-level cirrus clouds.

(ii) The individual cloud layers are mostly uncorrelated. This assumption enables us to neglect the effect of overlying clouds. Due to lack of adequate observational cloud data, we are unable to verify the validity of these two assumptions for the clouds present in the real world. Hence, we can not entirely rule out the possibility that the result obtained here for c_2 may only be a particular feature of the cloud model employed in the present analysis.

The two natural climate change experiments that the actual climate system performs are the zonal and seasonal climate change. Our conclusion that $c_2 \approx c_2(T_{sc})$ seems to apply to both of these climate change experiments since the data set we adopted includes summer, spring and winter values of temperature and humidity for low, middle and high latitudes. However, possible limitations of the present result to the actual climate system may arise due to the previously mentioned simplifying assumptions employed in the present model for treating the longwave radiative effects of clouds. It should also be pointed out that the c_2 values in Fig. 4 are obtained by placing the clouds in the troposphere and hence Eq. (7) is valid only for tropospheric clouds.

For reasons given below, the conclusion that $c_2 = c_2(T_{sc})$ should be applicable to WM's GCM: 1) the treatment of longwave effect of clouds adopted in the present analysis is similar to that of WM, and 2) we verified this conclusion by adopting WM's model values for the zonal temperatures.

Next, we will examine the effect of cloud-top feedback on the climate sensitivity of the model. Combining Eqs. (2), (5) and (7), we obtain

$$\frac{dF}{dT_s} = \frac{dc_1}{dT_s} - A_c\left(\frac{\partial c_2}{\partial T_{sc}}\right)\left(\frac{dT_{sc}}{dT_s}\right), \tag{8}$$

$$\beta = \frac{F_0}{\left(\frac{dc_1}{dT_s}\right) - A_c\left(\frac{\partial c_2}{\partial T_{sc}}\right)\left(\frac{dT_{sc}}{dT_s}\right) - \left[(S_0/4)\frac{d\alpha_p}{dT_s}\right]}. \tag{9}$$

Noting, first, from Fig. 4 that $(\partial c_2/\partial T_{sc})>0$, we conclude from Eqs. (8) and (9) that the sign of the cloud-top feedback depends on the sign of (dT_{sc}/dT_s). When $(dT_{sc}/dT_s)<0$ (or >0) the cloud top has a negative (or positive) feedback effect since dF/dT_s increases (or decreases) and β decreases (or increases) in magnitude when compared to the case when $(dT_{sc}/dT_s)=0$. We will now indicate the potential importance of the cloud-top feedback with sample calculations. Let us consider globally averaged conditions for which $T_s \approx 288$ K, $A_c \approx 0.5$ and $z_c \approx 6$ km. Assuming a tropospheric lapse rate $(-dT/dz)$ of 6.5 K km^{-1}, $T_{sc}=39$ K. From Ramanathan (1976), $\partial c_1/\partial T_s = 2.1$ W m^{-2} K^{-1}, while from Fig. 4 $\partial c_2/\partial T_{sc} = 1.65$ W m^{-2} K^{-1}; introducing these values in Eq. (8) we obtain

$$\frac{dF}{dT_s} = 2.1 - 0.83\frac{dT_{sc}}{dT_s}. \tag{10}$$

From Eq. (10), we can obtain the following relations:

$$\frac{dF}{dT_s} = \begin{cases} 1.27, & dT_{sc}/dT_s = 1 \\ 2.10, & dT_{sc}/dT_s = 0 \\ 2.93, & dT_{sc}/dT_s = -1. \end{cases} \tag{11}$$

For the assumed values of (dT_{sc}/dT_s), we see that the cloud-top feedback can potentially be important. Incidentally, Eq. (11) also explains an interesting result obtained by Cess (1974). Cess (1974) has shown that the magnitude of dF/dT_s for the fixed cloud-top altitude (FCA) model is larger than that for the fixed cloud-top temperature (FCT) model by a factor of about 1.6. In the FCA model the cloud-top altitude is fixed as T_s is changed while in the FCT model the cloud-top temperature is held fixed as T_s is changed. In both the models the tropospheric lapse rate is fixed such that the tropospheric temperature changes uniformly with T_s. It then follows that $dT_{sc}/dT_s=0$ for the FCA model while $dT_{sc}/dT_s=1$ for the FCT model, and from Eq. (11) we infer that dF/dT_s for the FCA model should be larger than the FCT model by a factor of about 1.6 as indeed obtained by Cess. As explained below, the conclusion that the cloud-top feedback vanishes for the FCA model is valid only for the case for which the tropospheric lapse rate is fixed.

WM's GCM adopts the FCA model. Nevertheless,

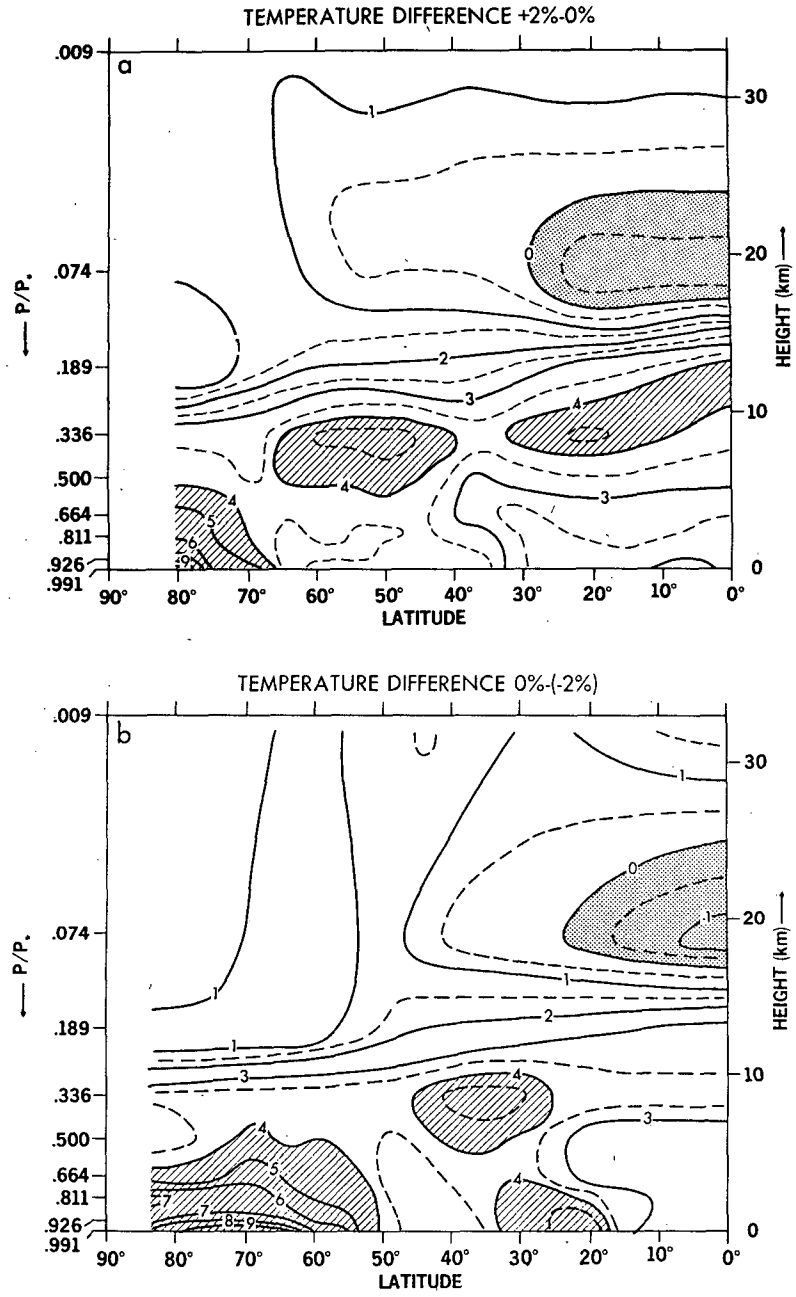

FIG. 5. Latitudinal profile of atmospheric temperature change resulting from a 2% increase (a) and a 2% decrease (b) in solar constant in the GCM (after Wetherald and Manabe, 1975). Fig. 5b was not shown in Wetherald and Manabe's paper and is shown here with the permission of Wetherald and Manabe.

because the tropospheric lapse rate changes in the model (as we will show later), the cloud-top feedback plays a major role in determining the magnitude of ΔT_s. In WM's model, as T_s increases the tropospheric lapse rate Γ decreases in low latitudes while Γ increases in high latitudes (see Fig. 3b in WM). To illustrate how changes in lapse rate influence the cloud-top feedback in the FCA model, we will assume that Γ is independent of altitude within the troposphere such that we can write

$$T_{sc}=T_s-T_c=\frac{T_s-T_c}{z_c-0}(z_c-0)=z_c\Gamma, \tag{12}$$

where $\Gamma=-dT/dz=$constant. Since z_c is constant in the FCA model, we can write

$$\frac{dT_{sc}}{dT_s}=z_c\frac{d\Gamma}{dT_s} \tag{13}$$

and upon combining Eqs. (10) and (13), we obtain

$$\frac{dF}{dT_s}=2.1-0.83z_c\frac{d\Gamma}{dT_s}. \tag{14}$$

From Eq. (14) we infer that in the FCA model the cloud-top feedback is negative in low latitudes (since $d\Gamma/dT_s<0$) and positive in high latitudes (since $d\Gamma/dT_s>0$). This completes our qualitative demonstration of the existence of the opposite effects of the cloud-top feedback in WM's model. Next, we will demonstrate quantitatively the major role played by cloud-top feedback in determining the nonlinear response of the latitudinal and global changes in T_s in WM's model.

b. *Analysis of GCM experiments*

Figs. 5a and 5b show the change in surface and atmospheric temperatures as a function of latitude and altitude, respectively, for experiments 1 and 2. These results were obtained by WM's GCM.

Several features immediately become apparent. The magnitude of ΔT_s is smallest at low latitudes and increases monotonically toward high latitudes. Further, we see that the lapse rate Γ decreases with an increase in T_s at low latitudes, while Γ increases at high latitudes. As explained in WM, the decrease in Γ at low latitudes is because Γ at low latitudes is determined largely by moist convective processes for which $d\Gamma/dT_s<0$. At high latitudes, vertical convective mixing is weak and hence the increase in T_s is concentrated to a shallow region close to the surface such that $d\Gamma/dT_s>0$. WM indicate that the larger increase in T_s at high latitudes is due to the combined effect of ice-albedo feedback and the weak vertical convective mixing near the surface.

Now we will reexamine WM's results after accounting for the effect of cloud-top feedback. From Eq. (14), we conclude that the cloud-top feedback is negative at low latitudes (since $d\Gamma/dT_s<0$ from Fig. 5) and positive at high latitudes (since $d\Gamma/dT_s>0$), while at middle latitudes it essentially vanishes (since $d\Gamma/dT_s\approx0$). To estimate the magnitude of the negative feedback effect we computed dF/dT_s at 10° latitude and at 40° latitude and obtained

$$\frac{dF}{dT_s}=\frac{dc_1}{dT_s}-\sum_{i=1}^{3}A_{ci}\frac{dc_{2i}}{dT_s}$$
$$=\begin{cases}2.27+0.82=3.09 \text{ for } 10^\circ \text{ latitude}\\ 2.10-0.02=2.08 \text{ for } 40^\circ \text{ latitude}\end{cases} \tag{15}$$

For these computations, we adopted the vertical distributions of temperature for 10° and 40° latitudes from the 0 and +2% case and the three-layer cloud model from WM and the relative humidity profile from Manabe and Wetherald (1967). The flux calculations were performed with Ramanathan's (1976) model. The value of dF/dT_s at 10° is larger by a factor of 1.5 than that at 40° and this difference is sufficient to account qualitatively for the factor of 1.5 difference in ΔT_s between 40° and 10° [note from Fig. 5 that $\Delta T_s(10^\circ)\approx2$ K and $\Delta T_s(40^\circ)\approx3$ K]. In Eq. (15) the contribution to dF/dT_s from clouds is shown

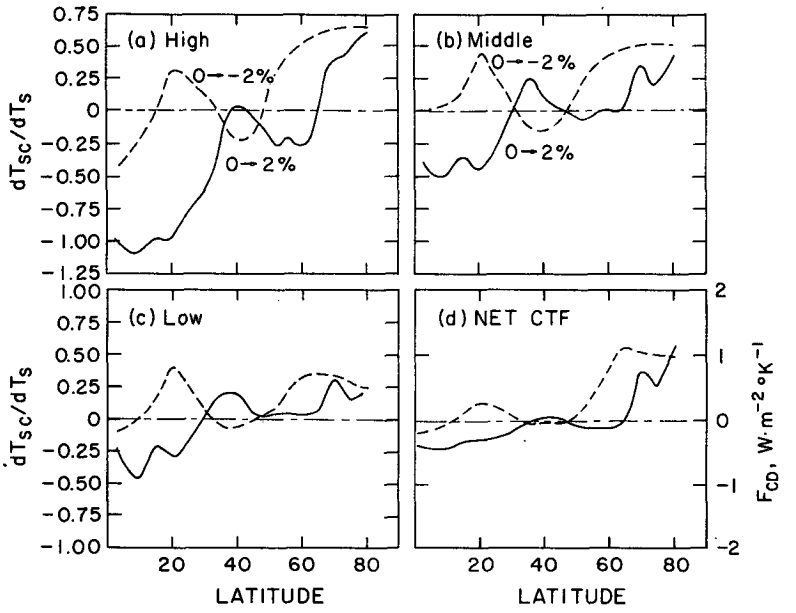

FIG. 6. Cloud-top feedback in GCM experiments. (a), (b) and (c) show values of dT_{sc}/dT_s for high, middle and low clouds, respectively, while (d) gives the net effect of cloud-top feedback (CTF) in GCM. See Eq. (18) for the definition of F_{CD}.

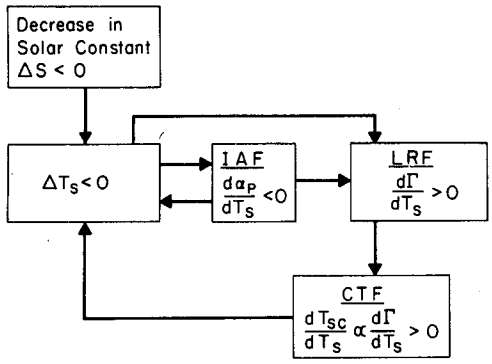

FIG. 7. A schematic illustration of the coupling between T_s, ice-albedo (IAF), lapse-rate (LRF), and cloud-top (CTF) feedbacks at high latitudes.

separately. We performed the same set of calculations for 80° latitude to estimate the positive feedback effect and obtain

$$\frac{dF}{dT_s}=1.7-0.48=1.22. \tag{16}$$

The second term on the right-hand side (16) is the contribution from the clouds. It will be seen later that the positive effect of cloud-top feedback contributes as much as the ice-albedo feedback to the ΔT_s at high latitudes. On comparing Eqs. (15) and (16), it is seen that the clear sky contribution to dF/dT_s also decreases from low to high latitudes, another point which will be discussed later.

As we concluded in the discussions following Eqs. (1), (2) and (3), the nonlinearity in $\Delta\bar{T}_s$ is introduced by the nonlinearity in the longwave sensitivity parameter. We will now show that the nonlinearity in dF/dT_s in WM's experiments is caused by the coupling between T_s, lapse-rate, ice-albedo and cloud-top feedback.

The latitudinal distribution of dT_{sc}/dT_s for experiments 1 and 2 is shown in Figs. 6a, 6b and 6c for high, middle and low clouds, respectively. The solid line corresponds to the $0\rightarrow+2\%$ case and the dashed line to the $0\rightarrow-2\%$ case. The dT_{sc}/dT_s values were calculated from Figs. 5a and 5b by letting $dT_{sc}/dT_s=\Delta T_{sc}(\theta)/\Delta T_s(\theta)$, where θ is the latitude. To evaluate the cloud-top temperature as a function of latitude, we adopted the latitudinal distribution of the three-level clouds given in Manabe (1969) since this distribution is adopted by WM.

Restricting our attention initially to the solid curves, we see that cloud-top feedback is negative (i.e., $dT_{sc}/dT_s<0$) at low latitudes and positive at high latitudes. This trend is exhibited by all three cloud levels. Comparing next the solid and the dashed curves, we see that, as the solar constant decreases, the region of negative feedback recedes toward low latitudes while the region of positive feedback expands toward mid-latitudes. The explanation for the expansion of the positive feedback toward mid-latitudes is straightforward. Since the positive feedback occurs when $d\Gamma/dT_s>0$, the expansion is due to a corresponding expansion of the region over which $d\Gamma/dT_s>0$. We give below possible reasons for the expansion of $d\Gamma/dT_s>0$. Over snow- or ice-covered regions, vertical convective mixing processes are small (due to sufficiently low values of T_s) and hence changes in T_s are confined to a shallow layer near the ground, resulting in $d\Gamma/dT_s$ being positive. Since the snow cover expands with a decrease in T_s, the $d\Gamma/dT_s>0$ (and hence positive feedback) region expands correspondingly. We feel this indirect coupling between ice-albedo and cloud-top feedback may be largely responsible for the expansion of positive cloud-top feedback. However, $d\Gamma/dT_s$ can be positive even in the absence of ice cover and hence all of the expansion may not be due to the ice-albedo feedback alone. A schematic illustration of the coupling between the various feedbacks is given in Fig. 7.

We now consider the receding of the negative feedback effect toward low latitudes as the solar constant is decreased. As mentioned earlier, the cloud-top feedback is negative when $d\Gamma/dT_s<0$ and $d\Gamma/dT_s<0$ in regions where moist convective processes determine Γ. It then follows that the receding of the negative effect of cloud-top feedback toward low latitudes implies the receding of the region dominated by moist convective processes toward low latitudes with a decrease in solar constant.

We will estimate the gobal effect of cloud-top feedback by considering the equation for the global longwave sensitivity parameter $d\bar{F}/d\bar{T}_s$ given by

$$\frac{d\bar{F}}{d\bar{T}_s}\approx\frac{\Delta\bar{F}}{\Delta\bar{T}_s}=\frac{\Delta\bar{c}_1}{\Delta\bar{T}_s}-\bar{A}_c\frac{\Delta\bar{c}_2}{\Delta\bar{T}_s}, \tag{17}$$

where $\bar{c}_1$, $\bar{c}_2$ and $\bar{A}_c$ denote globally averaged values. The term $\bar{A}_c(\Delta\bar{c}_2/\Delta\bar{T}_s)$, which denotes cloud-top feedback, may be written

$$\bar{A}_c\frac{\Delta\bar{c}_2}{\Delta\bar{T}_s}=\int_0^{90^\circ}F_{CD}(\theta)\cos\theta d\theta,$$
$$F_{CD}(\theta)=\Big[\sum_{i=1}^{3}\tilde{A}_{c,i}(\theta)\Delta c_{2,i}(\theta)\Big]/\Delta\bar{T}_s, \tag{18}$$

where θ is the latitude and the subscript i denotes the cloud level with $i=1$, 2, 3 denoting the low, middle and upper level clouds, respectively. $\tilde{A}_{c,i}$ is the fractional cloud cover that is not overlapped by the upper clouds, i.e., $\tilde{A}_{c,3}=A_{c,3}$, $\tilde{A}_{c,2}=A_{c,2}(1-A_{c,3})$ and $\tilde{A}_{c,1}=A_{c,1}(1-A_{c,2})(1-A_{c,3})$. The values of $A_{c,i}(\theta)$ are obtained from Manabe (1969). The term $\Delta c_{2,i}(\theta)$ is computed from

$$\frac{\Delta c_{2,i}}{\Delta\bar{T}_s}=\frac{\partial c_{2,i}}{\partial T_{sc,i}}\frac{\Delta T_{sc,i}}{\Delta\bar{T}_s}. \tag{19}$$

Note that in Eq. (19) $\partial c_{2,i}/\partial T_{sc,i}$ is a slight function of latitude and cloud-top altitude, because T_{sc} is a function of latitude and cloud-top altitude and as seen from Fig. 4 the value of $\partial c_2/\partial T_{sc}$ varies slightly with T_{sc}. $F_{CD}(\theta)$ was calculated by obtaining the value of $\partial c_{2,i}/\partial T_{sc,i}$ from Fig. 4 and the $\Delta T_{sc,i}/\Delta \bar{T}_s$ values from Figs. 6a, 6b and 6c. The computed values of $F_{CD}(\theta)$ are shown in Fig. 6d. From Fig. 6d we obtain

$$\int_{0^\circ}^{90^\circ} F_{CD}(\theta)\cos\theta d\theta = \begin{cases} -0.128 \text{ W m}^{-2} \text{ K}^{-1} & \text{for } S_0 \rightarrow S_0 + 2\% \\ +0.205 \text{ W m}^{-2} \text{ K}^{-1} & \text{for } S_0 \rightarrow S_0 - 2\% \end{cases} \quad (20)$$

Thus we see that cloud-top feedback has a net negative effect on the global sensitivity for $S_0 \rightarrow +2\%$ but a net positive effect with a decrease in the solar constant. Upon substituting the values of $\Delta\bar{F}/\Delta\bar{T}_s$ given in Table 1 and the values given by Eq. (20) for $\bar{A}_c\Delta\bar{c}_2/\Delta\bar{T}_s$ in Eq. (17), we can obtain $\Delta\bar{c}_1/\Delta\bar{T}_s$ for the two experiments. $\Delta\bar{c}_2/\Delta\bar{T}_s$ is obtained by dividing Eq. (20) by $\bar{A}_c$ (=0.51). The equation for $d\bar{F}/d\bar{T}_s$ is

$$\frac{d\bar{F}}{d\bar{T}_s} = \begin{cases} 1.94 + 0.25\bar{A}_c & \text{for } S_0 \rightarrow S_0 + 2\% \\ 1.8 - 0.4\bar{A}_c & \text{for } S_0 \rightarrow S_0 - 2\% \end{cases} \quad (21)$$

Since the change in the clear sky sensitivity is relatively smaller, Eq. (21) clearly shows that the significant change in $d\bar{F}/d\bar{T}_s$ between the two experiments (as shown in Table 1) is caused primarily by the sign of cloud-top feedback changing from negative to positive with a decrease in solar constant from $+2\%$ to -2%. The reason for the sign change is self-explanatory from Figs. 6a–6d. Thus we conclude that the nonlinear change in $\Delta\bar{T}_s$ between $S_0 \rightarrow S_0 + 2\%$ and $S_0 \rightarrow S_0 - 2\%$ experiments is caused by the change in sign of the cloud-top feedback which is due to the mutual coupling between T_s, lapse-rate, cloud-top and ice-albedo feedback and is not caused by the ice-albedo feedback alone.

c. *Nonlinearity in clear sky sensitivity*

From Eq. (21) we see that $d\bar{c}_1/d\bar{T}_s$ (i.e., clear sky sensitivity) decreases with a decrease in $\bar{T}_s$. Before we attempt to explain possible reasons for this, we will add the following word of caution. The $d\bar{c}_1/d\bar{T}_s$ term in Eq. (21) was not calculated from the model but was inferred from Eq. (17) and hence an error in our calculated values of F_{CD} may possibly have introduced an error. Nevertheless, independent model calculations indicate that $d\bar{c}_1/d\bar{T}_s$ should decrease with $\bar{T}_s$. We calculate

$$\frac{dc_1}{dT_s} = \begin{cases} 2.3, & \text{moist lapse rate } (d\Gamma/dT_s) < 0 \\ 2.07, & \text{fixed lapse rate } (d\Gamma/dT_s) = 0, \\ & \Gamma = 6.5 \text{ K km}^{-1} \\ 1.83, & \text{polar lapse rate } (d\Gamma/dT_s) > 0 \end{cases} \quad (22)$$

For all of the calculations, dc_1/dT_s was obtained by calculating c_1 at $\bar{T}_s$, $\bar{T}_s+\Delta T$, $\bar{T}_s-\Delta T$, where $\bar{T}_s = 288$ K and $\Delta T = 1$ K, and setting $dc_1/dT_s = c_1(\bar{T}_s) - c_1(\bar{T}_s - \Delta T)$. If the dc_1/dT_s obtained from this value is slightly different than $c_1(\bar{T}_s+\Delta T) - c_1(\bar{T}_s)$, then we take a linear average of the two dc_1/dT_s values. For the polar lapse rate case, we obtained $d\Gamma/dT_s$ from the vertical distribution of temperature difference at 75°N shown in Fig. 5. It is clearly seen that dc_1/dT_s is negatively correlated with $d\Gamma/dT_s$, i.e., we can write from Eq. (22)

$$\frac{dc_1}{dT_s} = c_1^0 - c_1' \frac{d\Gamma}{dT_s} \quad (23)$$

which is very much analogous to Eq. (14). In other words, the effective atmospheric radiating temperature, just as the cloud-top temperature, is coupled to the surface temperature through the lapse rate. Now, as discussed earlier in WM's experiments the region where $d\Gamma/dT_s > 0$ expands with a decrease in $\bar{T}_s$ while the region where $d\Gamma/dT_s < 0$ shrinks with a decrease in $\bar{T}_s$. Both of these effects tend to decrease dc_1/dT_s with a decrease in $\bar{T}_s$ as indeed shown by Eq. (21).

d. *Lapse-rate feedback*

From Eqs. (14) and (23), we see that dF/dT_s is negatively correlated with $d\Gamma/dT_s$. Coakley (1977) also obtains a negative correlation between dF/dT_s and $d\Gamma/dT_s$. Following Coakley (1977) we can write

$$\frac{dF}{dT_s} = \frac{\partial F}{\partial T_s}\bigg|_{\Gamma=\text{const}} + \frac{\partial F}{\partial \Gamma}\frac{\partial \Gamma}{dT_s}, \quad (24)$$

where, based on Eqs. (14) and (23), $\partial F/\partial T_s$ and $\partial F/\partial\Gamma$ can be written as

$$\left.\begin{aligned} \frac{\partial F}{\partial T_s} &= c_1^0 - \bar{A}_c c_2^0 \\ \frac{\partial F}{\partial \Gamma} &= -[c_1' + \bar{A}_c c_2'] \end{aligned}\right\}. \quad (25)$$

In the absence of the coupling between T_s and Γ, $\partial F/\partial T_s = dF/dT_s$. For the fixed cloud-top altitude model $c_2^0 \approx 0$. Both c_1' and c_2' are positive and hence Eqs. (24) and (25) clearly show the negative correlation between dF/dT_s and $d\Gamma/dT_s$. Since $d\Gamma/dT_s$ influences dF/dT_s which in turn feeds back into $\Delta\bar{T}_s$, we refer to the coupling between Γ and T_s as the lapse rate feedback. Thus, WM's model has effectively two feedbacks, lapse rate and ice albedo. The effect of the lapse-rate feedback on T_s is manifested through its contribution to clear sky and cloudy sky longwave sensitivity parameter. Its contribution to the cloudy sky longwave sensitivity gives rise to the cloud-top feedback in

TABLE 2. Comparison of zonal sensitivity: zonal sensitivity $=dT_s/d\bar{T}_s$.

Latitude	WM $S_0 \rightarrow S_0+2\%$	dF/dT_s (W m^{-2} K^{-1})	Present $\nu=2.2$ W m^{-2} K^{-1} Cloud-top feedback neglected	Cloud-top feedback included
85	3	$1.7-\bar{A}_c$ (0.81)	1.9	3.0
75	1.9	$1.78-\bar{A}_c$ (0.61)	1.11	1.3
65	1.1	$1.85-\bar{A}_c$ (0.22)	1.03	1.1
55	1.2	$1.9-\bar{A}_c$ (0.1)	0.98	1
45	1.26	$2.03-\bar{A}_c$ (0.02)	0.86	0.86
35	1.25	$2.16+\bar{A}_c$ (0.37)	0.92	0.86
25	0.73	$2.27+\bar{A}_c$ (0.6)	0.9	0.85
15	0.71	$2.35+\bar{A}_c$ (1.02)	0.92	0.81
5	0.65	$2.4+\bar{A}_c$ (1.45)	0.92	0.76

WM's model. It is important to realize that the cloud-top feedback can exist even in the absence of lapse-rate feedback since the term c_2^0 in Eq. (25) can be nonzero even when $d\Gamma/dT_s=0$. However, for the fixed cloud-top altitude model $c_2^0\approx 0$ and consequently in this model cloud-top feedback will essentially vanish if $d\Gamma/dT_s=0$. We should, however, caution that the preceding conclusion applies only for the clouds within the troposphere.

In the next section we will attempt to estimate the contribution of the ice-albedo, lapse-rate and cloud-top feedback to latitudinal temperature changes.

e. *The zonal sensitivity*

We will seek a simplistic approach to infer the relative importance of cloud-top, lapse-rate and ice-albedo feedback in determining the changes in zonal temperatures. The simplest climate model that can be used for this purpose is the zonal annual climate model which considers the zonal energy balance equation

$$S(\theta)[1-\alpha_p(\theta)]-F(\theta)=\nu[T_s(\theta)-\bar{T}_s], \qquad (26)$$

where $S(\theta)$ is the zonal solar insolation at the top of the atmosphere and α_p the zonal albedo of the earth-atmosphere system. The term on the right-hand side represents the poleward advection of heat, $T_s(\theta)$ is the zonal temperature, $\bar{T}_s$ the globally averaged surface temperature and ν the transport coefficient. Following Lian and Cess (1977), the ratio of the zonal and global sensitivity can be obtained from Eq. (26) in the form

$$\frac{dT_s}{d\bar{T}_s}=\frac{\nu+[S_0(\theta)/\beta][1-\alpha_p(\theta)]}{\nu+(dF/dT_s)+\{S_0(\theta)[\partial\alpha_p/\partial T_s]}\}. \qquad (27)$$

We adopted the values of Lian and Cess (1977) for $\partial\alpha_p/\partial T_s$ and the values of Ellis and Vonder Haar (1976) for $S_0(\theta)$ and $S_0(\theta)[1-\alpha_p(\theta)]$. The parameter β is defined by Eq. (1) and for the experiment 1, $\beta=150$. For the calculations of dF/dT_s as a function of latitude, we adopted the temperature profiles shown in Fig. 5. The results of the calculations are shown in Table 2 along with WM's results.

The value of $dT_s/d\bar{T}_s$ is calculated with and without including the cloud-top feedback. The calculated value of dF/dT_s is shown in the third column of Table 2. The results obtained without inclusion of the cloud-top feedback is shown in the fourth column. The effect of cloud-top feedback is neglected by deleting the term involving $\bar{A}_c$ in dF/dT_s. The results shown in the fourth column include the ice-albedo feedback and the effect of lapse-rate feedback on dc_1/dT_s, and the last column in Table 2 includes these feedbacks and cloud-top feedback. The value of ν chosen in the present analysis is smaller than Lian and Cess' value by 37%. The value of $\nu=2.2$ W m^{-2} K^{-1} was chosen to make the value of $dT_s/d\bar{T}_s$ at 85°N as obtained from the present analysis agree with WM's experiment. This procedure will enable us to examine the relative effects of ice-albedo and cloud-top feedbacks within the framework of WM's model experiments. The smaller value of ν may be justifiable since WM's model neglects ocean heat transport. However, we are not claiming that the parameter ν, which perhaps has no analogy to the real world, simulates the transport characteristics of WM's GCM.

A comparison of columns 4 and 5 of Table 2 shows the significant effect of cloud-top feedback in determining the latitudinal sensitivity. The last column predicts the qualitative trend of the latitudinal dependence of $dT_s/d\bar{T}_s$ obtained by WM. The results shown below summarize the relative effect of the various feedback mechanisms:

$$\frac{dT_s(85°\text{N})}{dT_s(15°\text{N})}=\begin{cases}3.94, & \text{case 1}\\ 2.06, & \text{case 2}\\ 1.6, & \text{case 3}\end{cases} \qquad (28)$$

Case 1 includes the ice-albedo feedback and the effects of lapse-rate feedback on dc_2/dT_s and dc_1/dT_s. Case 2 is the same as case 1 except that $dc_2/dT_s=0$. Case 3 considers only ice-albedo feedback. The influence of lapse-rate feedback on dF/dT_s is deleted in case 3 by assuming dF/dT_s to be independent of latitude and setting $dF/dT_s=d\bar{c}_1/d\bar{T}_s=2$ W m^{-2} K^{-1}. Hence case 3 indicates the contribution by ice-albedo feedback to ΔT_s at high latitudes. The contribution that results from the effect of lapse-rate feedback on dc_1/dT_s is seen by comparing cases 2 and 3, while the contribution by cloud-top feedback can be seen by comparing cases 1 and 2.

The positive effect of cloud-top feedback at high latitudes would have been much larger if WM had adopted the FCT model instead of the FCA model. At 85° latitude, we obtain $dF/dT_s=1.7-\bar{A}_c(1.65)$ for the FCT model and upon substituting this value

into Eq. (31) we have

$$\frac{dT_s(85°\text{N})}{d\bar{T}_s}=6.2, \quad \text{FCT model.} \tag{29}$$

Comparing this value with the value of 1.9 obtained by neglecting the cloud-top feedback (Table 2), it is seen that the sensitivity of the FCT model is larger by a factor of 3 than that of the model without the cloud-top feedback. The various cloud-top models discussed thus far indicate the options available to us for prescribing the cloud top in the models. Since there are no theoretical justifications to choose any one of these models as being more appropriate to the real world, we can only conclude that modeling assumptions concerning the cloud-top introduces a threefold uncertainty in the predicted values of ΔT_s at high latitudes.

3. The *e*-type absorption and the hydrological cycle

One of the important results of WM's experiments concerns the intensification of the hydrological cycle with an increase in solar constant. One of the reasons (as offered by WM) for the increase in the hydrological cycle is the decrease of the net longwave upward flux, F^N, at the surface with an increase in T_s. The upward flux at the surface can be written as

$$F^N=F_0-A_cF_C, \tag{30}$$

where

$$F_0=\sigma T_s^4-F_A^{\downarrow}, \tag{31}$$

$$F_C=F_C^{\downarrow}-F_A^{\downarrow}. \tag{32}$$

In the above equations, $F_A^{\downarrow}$ is the downward longwave flux emitted by the atmosphere under clear sky conditions and $F_C^{\downarrow}$ is the downward flux emitted by the cloud-cover portions of the atmosphere such that the term F_C in Eq. (30) is the correction to F^N due to the presence of clouds. WM show that, $dF^N/d\bar{T}_s<0$ and the negative sign implies that as T_s increases the longwave energy input to the surface increases and this increased longwave energy input leads to an increased H_2O evaporation which ultimately causes the intensification of the hydrological cycle. The negative dF^N/dT_s arises primarily because $F_A^{\downarrow}$ increases at a faster rate than σT_s^4 with an increase in T_s. The increase in $F_A^{\downarrow}$ arises from two effects: (1) the increase in atmospheric temperature and 2) the increase in H_2O amount associated with an increase in temperature. Since $d\Gamma/dT_s<0$ in low latitudes, we can intuitively expect that $-dF^N/dT_s$ would be larger in low latitudes (as indeed is the case). WM have shown that $-dF^N/dT_s$ is at a maximum at low latitudes and decreases toward mid-latitudes; in high latitudes $dF^N/dT_s>0$. For the globally averaged condition, WM obtain $dF^N/d\bar{T}_s<0$ which indicates that the contribution by the low latitudes determines the global value.

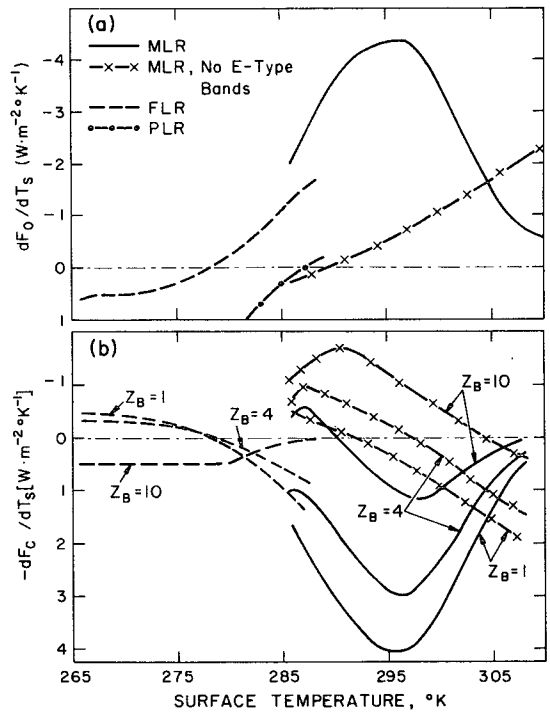

FIG. 8. Sensitivity of net surface upward longwave flux: (a) sensitivity of clear-sky fluxes F_0 and (b) sensitivity of the cloudy sky (overcast) contribution to upward flux (F_C). z_B denotes altitude of cloud bottom; MLR, moist lapse rate; FLR, fixed lapse rate; PLR, polar lapse rate.

Here, we would like to point out a potentially important contribution to $dF^N/d\bar{T}_s$ that arises from the *e*-type absorption by H_2O. The absorption coefficient K_ν of the H_2O continuum bands in the 8–12 μm and 17–21 μm regions can be written (Bignell, 1970)

$$K_\nu=K_{\nu 1}e+K_{\nu 2}P, \tag{33}$$

where e is the partial pressure of H_2O and P the total pressure. The *e*-type absorption refers to the absorption by the term $K_{\nu 1}e$. Since the optical depth τ is given by the product of K_ν and H_2O amount, it is seen that the emission by the *e*-type bands is proportional to e^2 while the emission by the other H_2O bands is proportional to e. This e^2 dependence enables the *e*-type bands to contribute significantly to dF^N/dT_s as shown in Figs. 8a and 8b. The results shown in the two figures were estimated by adopting Ramanathan's (1976) radiative transfer model. The symbol MLR denotes moist lapse rate, i.e., for the dF_0/dT_s calculations, the lapse rate in the adopted tropospheric temperature profile corresponds to the moist lapse rate. Similarly FLR denotes fixed lapse rate, i.e., $d\Gamma/dT_s=0$ ($\Gamma=6.5$ K km^{-1}) and PLR denotes polar lapse rate, i.e., $d\Gamma/dT_s>0$ and for this case we obtained $d\Gamma/dT_s$ from the value of $d\Gamma/dT_s$ at 75°N shown in Fig. 5. The model adopted for the curve marked "MLR, no *e*-type bands" is the same as that adopted

for the MLR curve except that the H_2O *e*-type bands were neglected in this set of calculations. Fig. 8a shows the clear sky sensitivity while Fig. 8b shows the contribution to this sensitivity from cloudy (overcast) skies with z_B the altitude of the base of the clouds; the term dF^N/dT_s can be obtained from these curves by letting

$$\frac{dF^N}{dT_s}=\frac{dF_0}{dT_s}-\sum_{i=1}^{3} A_{ci}\frac{dF_{c,i}}{dT_s}. \tag{34}$$

The significant influence of the *e*-type bands is clearly seen. Between the temperatures 290 and 300 K (typical of the low latitudes in WM's model) the *e*-type bands enhance the clear-sky sensitivity by factors ranging from 4 to 8. In addition the shape of the two curves is significantly different. Based on the results shown in Fig. 8, we suggest that the *e*-type bands will be important in determining the sensitivity of the hydrological cycle to changes in T_s. Comparing next the MLR, FLR and PLR curves, we notice the substantial difference in $-dF_0/dT_s$ between these three curves. This substantial difference indicates that the lapse-rate feedback can substantially influence the surface energy budget which in turn affects the hydrological cycle and the growth of snow or ice cover.

4. Summary and conclusions

The main conclusions of the present paper are summarized below. Conclusions 4)–6) are based on our analysis of WM's experiments concerning the effects of changing the solar constant on the climate of a general circulation model.

1) The longwave modification effect of clouds is largely dependent on T_{sc} $(=T_s-T_c)$, where T_s and T_c are the surface temperature and cloud-top temperature, respectively.

2) The sign and magnitude of cloud-top feedback is essentially determined by dT_{sc}/dT_s.

3) In the fixed cloud-top altitude model, $dT_{sc}/dT_s \propto d\Gamma/dT_s$ (Γ is the lapse rate); consequently, in this model the lapse-rate feedback gives rise to cloud-top feedback.

4) There is a strong negative correlation between dF/dT_s (F is the outgoing longwave flux) and $d\Gamma/dT_s$. Most of the contribution to the negative correlation is due to the coupling between $d\Gamma/dT_s$ and cloud-top feedback [see 3) above]. Thus, the lapse-rate feedback effect on T_s operates through the coupling between dF/dT_s and $d\Gamma/dT_s$.

5) The lapse-rate feedback effect on changes in T_s is negative at low latitudes and positive at high latitudes. Thus, interactions between T_s, ice albedo, lapse rate, clear sky and cloudy sky longwave radiative fluxes gives rise to a negative feedback at low latitudes and two positive feedbacks, i.e., ice albedo and lapse rate, at high latitudes.

6) The surface area over which the two positive feedbacks operate expands (shrinks) with a decrease (increase) in T_s and the surface area of negative feedback shrinks (expands) with a decrease (increase) in T_s. Consequently, the global climate sensitivity parameter β (for WM's GCM) increases (decreases) with a decrease (increase) in T_s which results in a nonlinear response of the model climate to changes in solar constant.

In conclusion, we caution the readers that the present analysis considers only partially one of the two important aspects of the cloud feedback problem. A full treatment of the cloud-top feedback problem would necessitate determining variations of cloud-top altitude with variations in T_s. We would also have to consider the feedback between cloud cover and T_s for a complete description and the net effect of clouds on T_s would depend on the combined effect of both cloud-top and cloud-cover feedback. However, the present analysis, although only providing partial answers, has demonstrated the magnitude of one important aspect of the cloud feedback problem.

Acknowledgments. I thank Drs. J. A. Coakley, R. E. Dickinson, W. W. Kellogg, S. Manabe and S. H. Schneider for their valuable comments on an initial draft of this paper. I am grateful to Mr. R. T. Wetherald for furnishing the temperature difference plots of his GCM solar constant experiments.

REFERENCES

Allen, J. R., 1971: Measurements of cloud emissivity in the 8–13 μm waveband. *J. Appl. Meteor.*, **10**, 260–265.

Bignell, K. J., 1970: The water-vapor infrared continuum. *Quart. J. Roy. Meteor. Soc.*, **96**, 390–403.

Cess, R. D., 1974: Radiative transfer due to atmospheric water vapor: Global considerations of the earth's energy balance. *J. Quant. Spectros. Radiat. Transfer*, **14**, 861–872.

——, 1976: Climate change: An appraisal of atmospheric feedback mechanisms employing zonal climatology. *J. Atmos. Sci.*, **33**, 1831–1843.

Coakley, J. A., Jr., 1977: Feedbacks in vertical-column energy balance models. *J. Atmos. Sci.*, **34**, 465–470.

Ellis, J., and T. H. Vonder Haar, 1976: Zonal average earth radiation budget measurements from satellites for climate studies. Atmos. Sci. Pap. No. 240, Colorado State University, 50 pp.

Hunt, G. E., 1973: Radiative properties of terrestrial clouds at visible and infrared thermal window wavelength. *Quart. J. Roy. Meteor. Soc.*, **99**, 346–369.

Lian, M. S., and R. D. Cess, 1977: Energy-balance climate models: A reappraisal of ice-albedo feedback. *J. Atmos. Sci.*, **34**, 1058–1062.

Manabe, S., 1969: Climate and the ocean circulation: I. The atmospheric circulation and the hydrology of the earth's surface. *Mon. Wea. Rev.*, **91**, 739–774.

——, and R. T. Wetherald, 1967: Thermal equilibrium of the atmosphere with a given distribution of relative humidity. *J. Atmos. Sci.*, **24**, 241–259.

McClatchey, R. A., R. W. Fenn, J. E. A. Selby, F. E. Volz and J. S. Garing, 1972: Optical properties of the atmosphere. Environ. Res. Pap. No. 411, Air Force Cambridge Research Laboratories [NTIS No. 0497].

Oort, A. H., and E. M. Rasmusson, 1971: Atmospheric circulation

statistics. NOAA Prof. Pap. No. 5. [U. S. Govt. Printing Office].

Platt, C. M. R., and D. J. Gambling, 1971: Emissivity of high layer clouds by combined lidar and radiometric techniques. *Quart. J. Roy. Meteor. Soc.*, **97**, 322–325.

Ramanathan, V., 1976: Radiative transfer within the earth's troposphere and stratosphere: A simplified radiative-convective model. *J. Atmos. Sci.*, **33**, 1330–1346.

Schneider, S. H., and R. E. Dickinson, 1974: Climate modeling. *Rev. Geophys. Space Phys.*, **12**, 447–493.

——, and C. Mass, 1975: Volcanic dusts, sunspots and temperature trends. *Science*, **190**, 741–746.

Wetherald, R. T., and S. Manabe, 1975: The effects of changing the solar constant on the climate of a general circulation model. *J. Atmos. Sci.*, **32**, 2044–2059.

Yamamoto, G., M. Tanaka and S. Asano, 1970: Radiative transfer in water clouds in the infrared region. *J. Atmos. Sci.*, **27**, 282–292.